

# TopGen: Topology-Aware Bottom-Up Generator for Variational Quantum Circuits

Jinglei Cheng<sup>†</sup> Hanrui Wang<sup>§</sup> Zhiding Liang<sup>‡</sup> Yiyu Shi<sup>‡</sup> Song Han<sup>§</sup> Xuehai Qian<sup>†</sup>

<sup>†</sup>Purdue University <sup>§</sup>Massachusetts Institute of Technology <sup>‡</sup>University of Notre Dame

Corresponding authors: cheng636@purdue.edu

**Abstract**—Variational Quantum Algorithms (VQA) are promising to demonstrate quantum advantages on near-term devices. Designing ansatz, a variational circuit with parameterized gates, is of paramount importance for VQA as it lays the foundation for parameter optimizations. Due to the large noise on Noisy-Intermediate Scale Quantum (NISQ) machines, considering circuit size and real device noise in the ansatz design process is necessary. Unfortunately, recent works on ansatz design either consider no noise impact or only treat the real device as a black box with no specific noise information. In this work, we propose to open the black box by designing specific ansatz tailored for the qubit topology on target machines. Specifically, we propose a bottom-up approach to generate topology-specific ansatz. Firstly, we generate topology-compatible sub-circuits with desirable properties such as high expressibility and entangling capability. Then, the sub-circuits are combined together to form an initial ansatz. We further propose circuits stitching to solve the sparse connectivity issue between sub-circuits, and dynamic circuit growing to improve the accuracy. The ansatz constructed with this method is highly flexible and thus we can explore a much larger design space than previous state-of-the-art method in which all ansatz candidates are strict subsets of a pre-defined large ansatz. We use a popular VQA algorithm – Quantum Neural Networks (QNN) for Machine Learning (ML) task as the benchmarks. Experiments on 14 ML tasks show that under the same performance, the TopGen-searched ansatz can reduce the circuit depth and the number of CNOT gates by up to  $2 \times$  and  $4 \times$  respectively. Experiments on three real quantum machines demonstrate on average 17% accuracy improvements over baselines.

## I. INTRODUCTION

Quantum computing is one of the most promising emerging techniques with great future potentials [3]. It exploits the exponential nature of quantum information processing, making it possible to solve the currently intractable problems such as integer factorization [69], chemistry simulations [43], quantum system simulation [72], [89] and large-scale database search [33], [40]. Significant breakthroughs have been made over the recent decades and different types of quantum computers have been implemented [15], [25], [42], [53]. However, the number of quantum bits (qubits) inside the quantum computers is still very limited. At the same time, the decoherence time of the qubits and gate fidelity seriously restrict the number of operations supported by the quantum machines. For these reasons, quantum computing is currently in the so-called Noisy Intermediate-Scale Quantum (NISQ) era [62]. The concept of *quantum volume* has been proposed to measure the capability of NISQ quantum computers [17]. Today, the most advanced quantum computers are composed of over 100 qubits [1] and the “quantum supremacy” has been

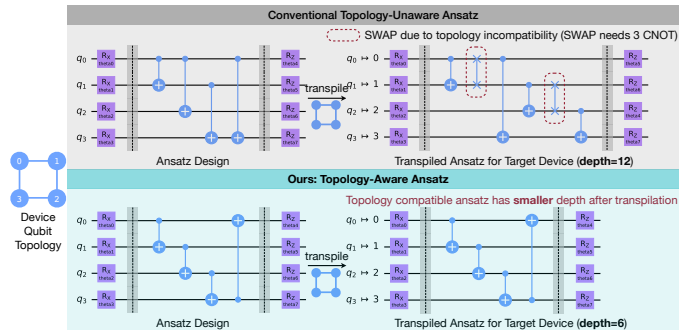


Fig. 1: TopGen *explicitly* considers the device topology, thus the transpiled ansatz has smaller depth.

recently demonstrated [27]. However, the targeting problem (random circuit sampling) is not practically useful.

A key characteristic of NISQ quantum computers is that the circuits are prone to decoherence, high gate errors and high measurement errors [6]. However, with elaborately developed quantum algorithms, we expect to see quantum supremacy in more areas such as Hamiltonian simulation [79] much sooner than other problems such as integer factorization [69]. *Variational quantum algorithms (VQAs)* are among the most promising candidates to show quantum advantage in the NISQ era. Examples of VQAs include variational quantum eigensolvers (VQE) [41], quantum approximation optimization algorithms (QAOA) [24] and quantum machine learning (QML) [9]. These algorithms typically contain *ansatz*, which is a variational circuit with parameterized gates that can be iteratively updated with classical optimizer to minimize the objective functions, i.e., approaching a certain desired state. They can be used to solve max-cut problems, find the ground state energy, and perform quantum chemical simulations [45].

Among the VQAs, the quantum neural network (QNN) [2] is gaining more and more attention due to its potential of representing complex data. Several QML models have been proposed to exploit quantum computers in practical use cases [34], [61], [86]. In QNN models, parametric quantum circuits are used as kernels to extract features from the input data set. Liu *et al.* [52] shows that for certain data sets with quantum nature, QML models can outperform the classical machine learning models.

For VQAs, the ansatz is a key component: different designs of ansatz will lead to very different performances. The metric for the performance depends on specific applications, it can

be either energy [49], [78] or accuracy [84]. The conventional approach of choosing ansatz depends heavily on the applications. For instance, hardware efficient ansatz [41] and UCCSD ansatz [7] are specially designed for VQE. The hardware efficient ansatz contains multiple layers of parameterized circuits. However, it has problems of trainability and barren plateaus due to its design with redundant gates. UCCSD ansatz captures the essence of the electron correlations in the molecule so it is a good approximation of the ground state of a molecular Hamiltonian [31]. For QNN, designing efficient ansatz with low cost and high accuracy is still an open problem.

Sim *et al.* [70] presented different ansatz derived or inspired by past studies such as hardware-efficient circuit [41], Josephson sampler circuits [26], Quantum Kitchen Sinks ansatz [85] and encoding circuits for QVECTOR algorithm [39]. This paper proposes a theoretical framework to characterize and compare parameterized quantum circuits based on two criteria: expressibility and entangling capability. There are also studies on how these properties affect the performance of the ansatz [36]. A strong correlation between classification accuracy and expressibility is found. A weak correlation between the entangling capability of a circuit and its classification accuracy is validated.

Some recent works [82], [90] adopted neural architecture search (NAS) [60] in classical machine learning to optimize the ansatz for QNN. Wang *et al.* [82] propose to search the good ansatz by iteratively sampling a super-circuit. The evolutionary search is performed to obtain the ansatz (sampled from super-circuit) with the best estimated performance. The performance estimation is conducted by using circuit simulations on noise-aware quantum simulators. Our method is fundamentally different from QuantumNAS. Firstly, QuantumNAS only considers the real machine as a black box and *implicitly* considers the qubit mapping during the search so the additional SWAP gates cannot be avoided for their searched circuits. On the contrary, our method considers the real machine as white box by *explicitly* designing sub-circuits with no need for SWAP insertions. Secondly, the design space of QuantumNAS is limited to subspace of a constructed SuperCircuit while ours can arbitrarily grow the ansatz. Zhang *et al.* [90] accelerated the process by training an RNN neural predictor to establish the correlation between circuit architecture and circuit performance, instead of relying on a simulator. Based on the results, the quality of the ansatz generated by the NAS based approach is superior to the ones manually designed such as hardware-efficient ansatz and the ansatz with replicated layers. In [83] and [51], authors propose frameworks to mitigate the qubit noise during the learning process. The method of weights pruning has also been introduced into the optimization of ansatz by recent work [71].

### Challenge in NISQ Machines

**Problem 1: mapping overhead.** All current attempts to optimize the ansatz are mainly focused on reducing ansatz size and improving model accuracy. However, the topology information of underlying quantum hardware is rarely considered. In the compilation workflow of quantum programs

such as QNN, the ansatz will eventually be mapped onto the physical qubits in quantum machines. Due to the sparse connection of the physical qubits, it is realized by inserting many SWAP gates into the original circuit. The process of compiling the circuit to match the topology of a specific quantum device is referred to as transpilation. We observe an average of 30% increase of circuit depth after compilation for 4-qubit hardware-efficient ansatz. The proportion of additional SWAP gates depends heavily on the circuit structure and the hardware topology. And it will generally be increased for larger circuits due to the sparser connections between physical qubits. It also affects the NAS based approaches, because the best ansatz selected considering ansatz size and accuracy may not be the best when the necessary SWAP gates are inserted during mapping.

**Problem 2: search overhead.** Generating ansatz candidates for NAS is challenging because the search space for such circuit is extremely large—growing exponentially with the number of gates in the circuit. For a complete ansatz with eight qubits and 40 gates, it is almost impossible to generate a “good” ansatz of such size by simply assigning random parameterized gates. The current NAS approaches use a top-down approach, i.e., generating ansatz by sampling the super-circuit, in which each ansatz candidate is still constrained by the super-circuit. This approach inherently incurs the mapping overhead because the super-circuit is oblivious to the hardware topology. Generating ansatz from scratch in a bottom-up fashion has the potential to consider hardware topology earlier and eliminate such overhead, however performing that without the super-circuit will be more difficult.

**Drawbacks of state-of-the-art approach** Recent works [29], [32], [76], [80], [82] have proposed different methods to tackle the challenges stated above. However, they have different drawbacks and limitations respectively. Adapt-VQE [32] has demonstrated the effectiveness of a “growing” algorithm in VQE task. The appended circuits originate from the Pauli operator with the largest gradient during the training process. The growing algorithm designed in adapt-VQE requires prior knowledge about the desired quantum states, which corresponds to the molecule’s lowest energy state. Namely, there exists a guided way to generate a good ansatz for VQE, as demonstrated by the golden standard UCCSD [31]. Machine learning tasks such as image classification are addressing more complicated problems, where we have nothing similar to Pauli operators from VQE algorithm. Namely, we have no prior knowledge on what the optimal ansatz would be. In this case, adapt-VQE cannot be adopted to find the optimal ansatz. Therefore, we need to search for better ansatz architectures. Besides, adapt-VQE evaluates its ideas with numerical simulations, whereas we test our methods on real-world quantum devices and validate the improvements shown in simulation results. QuantumNAS [82] provides a top-down method to create the ansatz circuits. The ansatz circuits are extracted from super-circuits with iterative evaluations, where extra computation overhead is introduced. To mitigate the drawbacks and limitations of

these approaches, we provide our solution TopGen to find better ansatz for QNN.

**Our solution: a bottom-up approach based on sub-circuits:** In this paper, we propose TopGen, a novel approach that addresses both problems at the same time. Instead of performing NAS from scratch at the gate level, we start from the *sub-circuits* as the building blocks to narrow the search space, making the optimization problem more tractable. The sub-circuits are aware of the qubit topology as shown in Figure 1. This approach can avoid the mapping overhead by ensuring quantum hardware-compatibility of the sub-circuits *by design*, i.e., there is no need to insert SWAP gates to the best ansatz generated. It can ensure good accuracy by generating sub-circuits with “good” properties, which can be measured by the expressibility and entangling capability as in [36]. With this approach, the search cost is the cost of generating the set of “good” sub-circuits. The size of the sub-circuits can naturally explore the trade-off between the quality and cost of the search. If the sub-circuits are too small, they cannot fully explore the Hilbert Space. With limited search space, we may fail to generate and find the ansatz that is good enough. On the other side, if the sub-circuits are too large, we will suffer the similar challenge of the giant search space as for the current NAS based approaches.

The effectiveness of this approach comes from the flexibility of QNN ansatz. Because the optimal ansatz does not have physical meaning, the final states of the ansatz can be from the full Hilbert Space. In comparison, the space of circuit synthesis for other quantum programs is much smaller than that of QNN programs because the physical meaning is reflected in the ansatz design. For example, the ideal ansatz for VQE is the approximation of the lowest energy states. The recent experimental results [82], [83], [90] confirmed such flexibility, showing that different properly designed ansatz can all reach decent accuracy. The flexibility and large search space indicate the potential of considering quantum hardware topology information in ansatz design. Our results show that the ansatz generated with our sub-circuit based approach can reach better accuracy with less number of gates and latency.

**Contribution.** The goal of this paper is to find the better architecture for QNN ansatz and demonstrate in both simulator and real NISQ machine. To realize the sub-circuit based bottom-up approach, we propose the following steps.

- **Sub-circuit generation.** We generate a group of sub-circuits that are compatible with hardware topology. Different gates are randomly selected and inserted to form the sub-circuits. The quality of sub-circuits are measured by the expressibility and entangling capability.
- **Ansatz construction.** After a library of sub-circuits is generated, the sub-circuits are used as building blocks to construct ansatz. The ones with superior performance will be selected and combined to generate an initial version of the QNN ansatz.
- **Optimizations.** It is likely that the initial combined ansatz does not reach the required accuracy. We propose several techniques to recover the accuracy loss by extending the

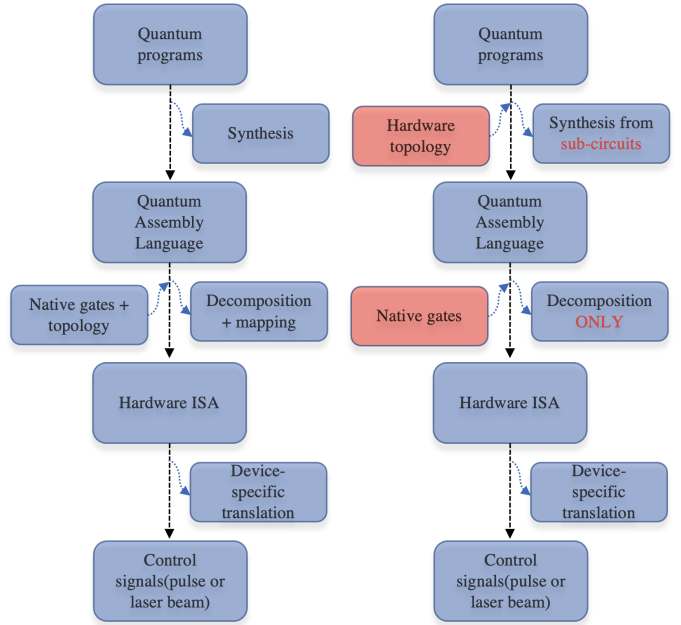


Fig. 2: Current compilation workflow for quantum programs compared with the proposed approach. In TopGen, the hardware topology is considered during synthesis. Therefore, the ansatz needs no extra SWAP gates after the program is synthesized.

ansatz: “stitching” the sub-circuits to enhance the entanglement; “growing” the ansatz to improve accuracy; and pruning the gates with small parameters to reduce ansatz size without affecting accuracy.

**Evaluation highlights.** We evaluated our approach with 14 data sets used in recent works. The results demonstrate that sub-circuits of better properties can help improve the performance of the combined ansatz. The ansatz generated by our approach achieves an average of 13% and 7% accuracy improvement over random ansatz and manually designed ansatz, respectively. The sizes of the generated ansatz are similar to baselines before compilation. But thanks to the hardware compatibility, after compilation, we observe around 50% reduction in circuit depth and up to 75% reduction in the number of CNOT gates.

## II. BACKGROUND

### A. Quantum Compilation Workflow

Quantum programs need to be compiled before being executed on quantum hardware. The programs are first translated into the quantum assembly language such as OpenQASM [18]. After the program is composed into only single-qubit and two-qubit gates, the mapping algorithm will insert SWAP gates into the quantum circuits to ensure that the program is compatible to the hardware topology of a specific quantum computer. Since the basic gates used in OpenQASM are usually different from the native gates supported by quantum computers. The quantum circuits need to be further decomposed into native

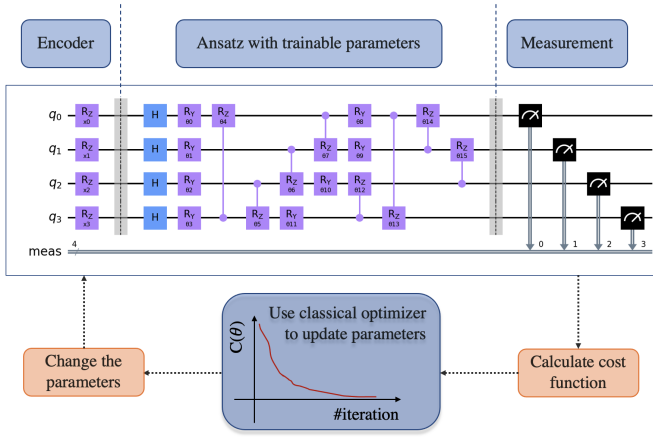


Fig. 3: QNN programs are composed of several parts: data encoder, ansatz, measurement and classical optimizer. In each iteration, the gradients of the parameters are calculated and the parameters are updated.

gates. In different quantum computer systems, the final transitions from native gates to control signals are different. For IBM quantum computers, the control signals for superconducting qubits are microwave pulses. IBM provides Qiskit [5] as a software development kit (SDK), in which the transpilers inside Qiskit correspond with the compilation workflow, including mapping, gate decomposition, etc. The traditional workflow is shown on the left of Figure 2.

### B. Variational Quantum Algorithms

In the NISQ era, VQAs are among the most promising approaches to achieve quantum supremacy for practical problems. Typically, VQA is a hybrid quantum-classical algorithm that uses classical optimizer to find the parameters  $\theta$  that minimize the cost function  $C(\theta)$ .

$$\theta^* = \underset{\theta}{\operatorname{argmin}} C(\theta). \quad (1)$$

The key idea of VQAs is to encode the problems into a cost function such that the minimum of the cost function corresponds to the solution of the problem. In general, the cost function can be defined as:

$$\theta = \sum_k f_k(\{\rho_k\}, \{O_k\}, \{U(\theta)\}) \quad (2)$$

where  $f$  is a function,  $U(\theta)$  is the parameterized circuits (ansatz),  $\rho_k$  represents inputs from the training set,  $O_k$  are the observables for measurements.

For example, in quantum chemistry, the variational method is a classical method to find low energy states of the quantum system. A trial wave function (ansatz) is defined with parameters. The expectation of the energy changes as the parameters vary. Then we can use classical optimizer to search for the minimum energy. The minimized ansatz is the approximation of the lowest energy states, and the corresponding energy

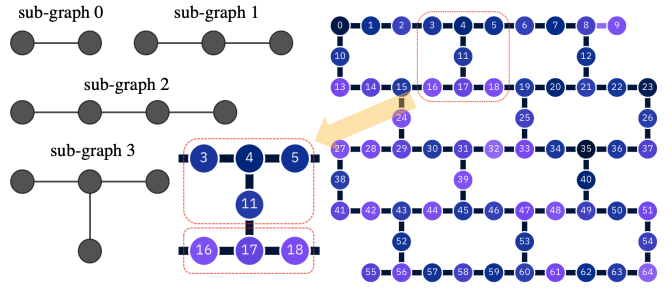


Fig. 4: Hardware topology of a real-world quantum computer `ibm_ithaca` [1]. The topology information is considered when sub-circuits are generated based on 4 sub-graphs shown in the figure.

gives an upper bound on the actual ground energy. In QML problems, however, the resulting minimized ansatz does not have physical meaning. It leads to a larger space to design the QML ansatz.

### C. Quantum Neural Network

QNN is a subset of VQAs that is composed of encoder, ansatz, decoder, etc. Abbas *et al.* [2] claims that the well-constructed QNNs can have substantially higher effective dimensions than classical neural networks, meaning that they can model a broader class of functions. In another word, QNN can achieve better performance than the comparable classical feedforward neural networks. Importantly, the benefit comes without the cost of reduced trainability. Figure 3 shows the basic structure of the QNN programs. The quantum circuits used in QNN contains an encoder and an ansatz, i.e., variational quantum circuits with trainable parameters. The input features are encoded inside the encoder gates as phase or amplitudes of rotations. These gates act as preliminary part for the ansatz. After the QNN circuits are combined, the measurements are performed, and we can obtain an output distribution. The value of the cost function is updated according to the output distribution. Gradients of the parameters are calculated with the parameter shift rule [16] and the trainable parameters are updated accordingly.

### D. Topology of Quantum Hardware

In currently available quantum devices, the quantum bits are usually not fully connected. The quantum bits are often arranged as 1-dimensional array or 2-dimensional grid-like or heavy-hexagon arrays. The connection between quantum bits is actually very sparse compared with the full connection. For example, `ibm_ithaca` is a 65-qubit quantum machine, but the total number of connections is 72 as shown in Figure 4. As a result, when the quantum programs are executed on the quantum machines, a considerable number of SWAP gates are inserted to the original quantum circuit to compensate for the sparse connection. We tested several 4-qubit quantum programs on the real-world hardware topology `ibmq_quito` [1]. We found that the mapped program has around 30%

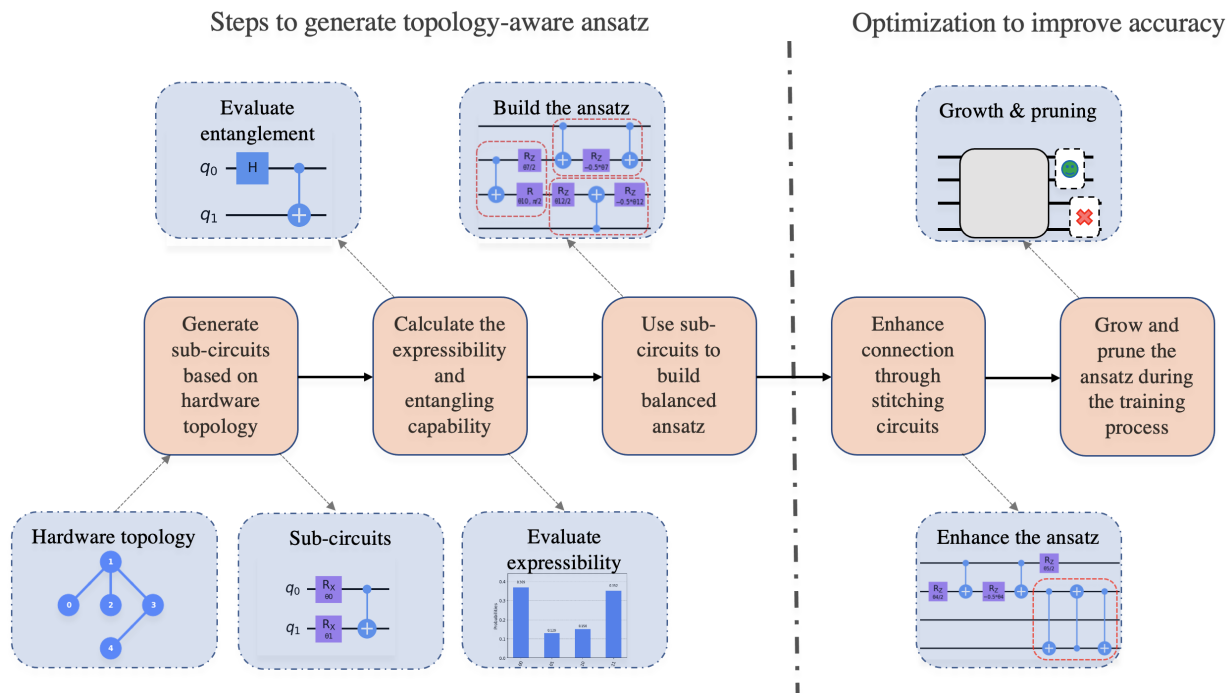


Fig. 5: Overview of the Proposed Approach: (1) Sub-circuits are generated based on hardware topology; (2) The circuits are evaluated with two criteria; (3) Sub-circuits are used as building blocks to generate an initial ansatz; (4) After the sub-circuits are concatenated together, additional two-qubit gates are added to boost the entanglement; (5) Ansatz is appended with small sub-circuits and trained to further improve accuracy.

more gates, and the circuit depth is increased by 40%. Such overheads vary from programs to programs. In general, we expect that the number of extra SWAP gates will become larger in near future, due to the increasing sparsity of physical qubit connections.

### III. PROPOSED BOTTOM-UP APPROACH

#### A. Motivation

With the current approaches, the mapping process is performed after the quantum circuits are synthesized. The quantum hardware topology is not considered during synthesis. As discussed earlier, it introduces additional overhead due to the inserted SWAPs, and affect the selection of proper ansatz for NAS. Intuitively, considering hardware topology during synthesis has the potential to generate better ansatz with less circuit depth. It is not possible with the current top-down NAS approach that generates the ansatz candidates from a topology-oblivious super-circuit. A straightforward solution is to generate the ansatz from scratch, and ensure that each generated ansatz is compatible to the hardware topology. However, this approach will lead to huge design space and requires very high computational resource to search for the ansatz. Conceptually, there is a *gap* between generated ansatz and hardware topology.

#### B. Sub-circuit as Building Blocks

To close this gap and make the optimization problem tractable, we propose *TopGen*, a *bottom-up approach using sub-circuits with compatible topology as the building blocks* to generate the ansatz for QNN. For a given quantum computer, the ansatz can be generated by combining the set of compatible sub-circuits—the sub-graphs corresponding to the sub-circuits can be embedded in the graph corresponding to the hardware topology. By design, the combinations of the sub-circuits require no extra SWAP gates in the mapping process. In our approach, the search of a huge design space is reduced to finding better sub-circuits that can form the high quality ansatz.

We use two criteria to evaluate the sub-circuits based on their capabilities to explore the Hilbert Space. The circuits are ranked and grouped according to their size and performance. The details are discussed in Section IV-B. Then the sub-circuits can be combined together to form an initial QNN ansatz. Since it is composed of multiple independent blocks, further optimizations are likely to be achievable. We propose several methods to boost the performance. First, after the sub-circuits are combined, we can add more two-qubit gates to compensate for the connection loss between the qubits. Second, during the training process, we “grow” the ansatz by appending small sub-circuits. This step terminates when no further reduction of the cost function is observed. Third, we

---

**Algorithm 1** Procedure to generate a sub-circuit

---

**Require:** Topology information, limit on circuit depth

- 1: Check available two-qubit connections from topology information and generate a set of compatible gates
  - 2: The set contains 1-qubit gates on all available qubits and 2-qubit gates on all available connections
  - 3: **while** Circuit depth  $\leq$  depth limit **do**
  - 4:   Select a random gate from the set
  - 5:   **if** The gate is not the same gate with the last gate **then**
  - 6:     Assign the gate to the qubit with least gates
  - 7:   **end if**
  - 8:   Update #gates on each qubit
  - 9: **end while**
  - 10: Set gate parameters to zeros
  - 11: **if** The resulting Unitary equals identity matrix **then**
  - 12:   The sub-circuit is labeled as appendable
  - 13: **end if**
  - 14: **return** One sub-circuit
- 

adopt the idea of dynamic pruning [71] to further reduce the size of the ansatz. Specifically, the gates with parameters that are close to zero are deleted. This step terminates if a sharp decrease of model accuracy is observed. The details of the search and optimization process are discussed in Section V.

In our approach, the reduction in search space may sacrifice some opportunity to find the optimal solution. However, given the huge search space for a bottom-up approach, the trade-off is worthwhile to make the optimization problem tractable. In our evaluation, QNNs are constructed and tested on various learning problems. The results show that our approach can generate QNN ansatz with similar—sometimes even better—accuracy compared to the state-of-the-art solutions with significantly reduced circuit size. Specifically, under similar performance, we achieved around 50% reduction on circuit depth and up to 75% reduction on the number of CNOT gates.

### C. Why Does It Work?

Classical machine learning and variational algorithms in quantum mechanics share similar mathematical structure [74]. Many natural quantum systems satisfy the area law of entanglement, which implies that the entanglement entropy scales as the surface area of the subsystem rather than its volume [23]. For example, the *ground states* of many typical Hamiltonians satisfy the area law [63], indicating that the relevant physics only takes place in a restricted part of the full Hilbert space. Our solution is inspired by the phenomenon of the area law: it is possible that we do not need to search in the full Hilbert space as QNN ansatz. Our solution explores such “locality” with the bottom-up approach. Our experimental results indeed suggest that local optimizations of sub-circuits can help improve the global performance.

## IV. SUB-CIRCUIT SELECTION

### A. Generating Sub-circuits

The SWAP gates are needed whenever the topology of a quantum circuit is different from the quantum computer topology. Typically, the connections between physical qubits are sparse for superconducting quantum computers, as shown in the example of Figure 4. For a given quantum computer, we consider the hardware topology as a connected graph, where qubits are vertices and available connections are edges. For the `ibm_ithaca`, we select 4 sub-graphs as bases to make our ansatz. Since the smallest sub-graph 0 contains only 2 qubits, only single isolated qubit can be uncovered in the worst case. For example, we want to design a 7-qubit ansatz. We can first select the 7 qubits from the quantum hardware, then divide the 7 bits into sub-graphs of size 3 and 4, as shown in Figure 4. If any uncovered single qubit exists, we can apply stitching circuits on it to connect isolated sub-graphs.

Based on the allowed sub-circuit topologies, we can generate small blocks of variational circuits that are compatible with the native quantum hardware topology. Such circuits are small in the aspect of width, depth and the number of parameters. The gate set for sub-circuits to choose from is  $\{CNOT, R_x(\theta), R_y(\theta), R_z(\theta)\}$ . The gate set can be extended to include  $\{\sqrt{X}, H\}$  gates as well. The controlled rotation gates can be decomposed into these gates, so it is excluded from the gate set. We also notice that  $R_x$  and  $R_y$  gates can be further decomposed into  $R_z$  gates and  $\sqrt{X}$  gates. We decide to include the single-qubit rotation gates, since their combinations can boost the expressibility better than random combination of  $R_z$  gates and  $\sqrt{X}$  gates.

With the topology information from quantum device, we can easily form a set of compatible gates. For example, if the quantum computer has the connection between qubit 0 and qubit 1, then compatible gates are 1-qubit gates and 2-qubit gates on qubit 0 and 1. To be more specific, 1-qubit gates are  $\{R_x(\theta), R_y(\theta), R_z(\theta)\}$  on both qubits; 2-qubit gates are  $\{CNOT(0, 1), CNOT(1, 0)\}$ . Therefore, the two-qubit gates are assigned only to available physical qubit connections. We notice that two identical rotation gates are the same as one rotation gate with parameter that is the sum of two separate parameters; and two consecutive CNOT gates form an identical matrix. Consequently, when compatible gates are assigned onto qubits, consecutive identical gates will be omitted.

The algorithm to randomly generate sub-circuit is shown in Algorithm 1. After generated, the sub-circuits are ranked with their performance (to be defined in the next section). The top sub-circuits are saved in the library for constructing QNN ansatz. During the process of sub-circuits generation, we divide the sub-circuits into two groups: the circuits that result in identity matrix with the parameters set to zeros; and the rest ones. The reason for grouping is to identify the sub-circuits that are suitable for proposed optimization method, more details will be discussed in Section V-C.

### B. Sub-circuits Quality Criteria

After the sub-circuits are generated, we measure the properties of them using the *expressibility* and the *entangling capabilities*. These properties are chosen as main criteria

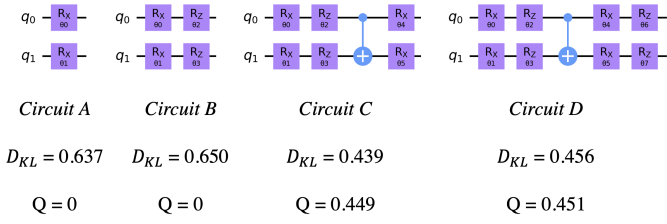


Fig. 6: Sub-circuit examples: from left to right, the circuits are larger with better expressibility and entangling capability.

since [36] demonstrates that they are highly correlated with the model accuracy. We expect to see better model accuracy with ansatz of better properties.

**Expressibility** It is defined as a circuit’s ability to generate states that well represent the Hilbert Space [70]. In the case of single-qubit system, it can be interpreted as how uniformly the Bloch Vectors are distributed on the Bloch sphere. To quantify the expressibility, we use the Kullback-Leibler (KL) divergence [44] to measure the difference between two distributions:  $Expr = D_{KL}(\hat{P}_{ansatz}(F; \Theta) || P_{Haar}(F))$ , where  $\hat{P}_{ansatz}(F; \Theta)$  describes the distribution of estimated fidelities  $F = |\langle \psi_\theta | \psi_\phi \rangle|^2$  with randomly sampled parameter pairs  $(\theta, \phi)$ .  $P_{Haar}(F)$  stands for the uniform distribution of states.  $P_{Haar}(F)$  can be derived in theory. Therefore, in experiments we only need to measure the distribution of  $\langle \psi_\theta | \psi_\phi \rangle$ .

Figure 6 shows examples of sub-circuits computational expressibility. For circuit A, only  $R_x$  gates are applied, the degree of freedom is very limited. Thus, the fidelity distribution will be very different from the uniform distribution. To quantify the difference, KL divergence is applied. For circuit C, where different rotation gates and CNOT gates are applied, the quantum states will explore the Bloch spheres more thoroughly. The distribution of the fidelity should be closer to the uniform distribution. Hence, we expect to see better expressibility for ansatz with more parameterized gates. On the other side, the sheer inclusion of parameterized quantum gates can lead to problems like barren plateaus [54] and trainability [77]. Thus, we need to limit the size of the ansatz to avoid such problems.

**Entangling capability** For QNN algorithms, the solution space for data classification tasks needs to be efficiently represented. In this context, the entangling capability provides potential advantages in capturing the non-trivial correlations in the datasets [70]. During the process of generating the sub-circuit library, the entangling capability is quantified by the Meyer-Wallach (MW) entanglement measure [55]. It is a global measure of multi-qubit entanglement for quantum states. While there are other methods for quantifying the entanglement, MW is generally more scalable and easy to compute:  $Q(|\psi\rangle) = 2(1 - 1/n \sum_{k=0}^{n-1} Tr[\rho_k^2])$ , where  $\rho_k$  is the one-qubit reduced density matrix of the k-th qubit after tracing out the rest [12]. The values of Q range from zero (no entanglement) to one (strong entanglement). This equation illustrates the physical meaning of such measure: it is an

---

## Algorithm 2 Combination of sub-circuits

---

**Require:** Hardware topology, evaluated sub-circuits

- 1: Select sub-circuits of best expressibility or best entanglement to build the ansatz
  - 2: **while** Circuit depth  $\leq$  depth threshold **do**
  - 3: Assign the sub-circuits to the physical qubit with least gates or assign the sub-circuits in the order of decreasing size
  - 4: Update #gates on each qubit
  - 5: **end while**
  - 6: **return** An initial QNN ansatz
- 

average over the entanglements of each qubit with the rest of the quantum system. If we measure the MW for bell state,  $|\psi\rangle = \frac{1}{\sqrt{2}}(|00\rangle + |11\rangle)$ , we will obtain  $Q = 1$ .

To evaluate the entanglement capability, multiple sets of random parameters are applied to the sub-circuit, and the corresponding  $Q$  values are calculated. We define the MW entanglement for the sub-circuit as the average value of  $Q$ . In Figure 6, for circuit A and B, different qubits do not interact (not entangled). The MW measure will return 0 for such situations. For circuit C and D, the two qubits are entangled through CNOT gates. Because they are parameterized circuits, the value of  $Q$  changes as parameters change. The displayed values are calculated by averaging a large number of quantum circuits with randomly sampled parameters. The MW entanglement measure has one drawback: it cannot distinguish two quantum states with very high entanglement because the MW entanglement measure will saturate. Fortunately, this drawback does not affect our evaluation of the sub-circuits. Because we calculate the *average* of  $Q$  values for different sets of parameters, although it is possible that  $Q = 1$  for *one* set of parameters, it is highly unlikely that  $Q = 1$  for *all* possible sets of parameters. Later in Figure 12, we can see that the MW measure of some ansatz are 0, but it is almost impossible that we experience entanglement saturation, i.e., obtaining 1 for MW measure. We notice that the Q values will saturate with more CNOT gates, which actually fits our principles. Since we want to limit the size of the circuits to narrow down the design space.

## V. SEARCHING HIGH ACCURACY ANSATZ

### A. Combining Sub-circuits

After obtaining a library of sub-circuits, we combine them to produce an initial ansatz. We give options to combine the circuit, for example, we can assign the sub-circuits onto the compatible qubit with least gates. The consequent ansatz would be balanced in terms of gates per qubit. We also allow to assign the sub-circuits in the order of their sizes. In this case, the ansatz is similar to traditional neural network with layers of decreasing dimensions. We observed negligible accuracy change among different combination methods. Thus, we choose the simple method to form a balanced initial ansatz. The assignment of sub-circuits ends when a threshold of depth

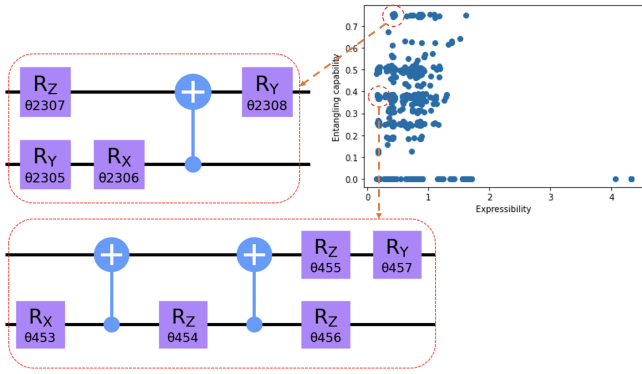


Fig. 7: Two sub-circuits are selected according to their great expressibility and entangling capability respectively. The combination generates a 4-qubit ansatz with 12 gates.

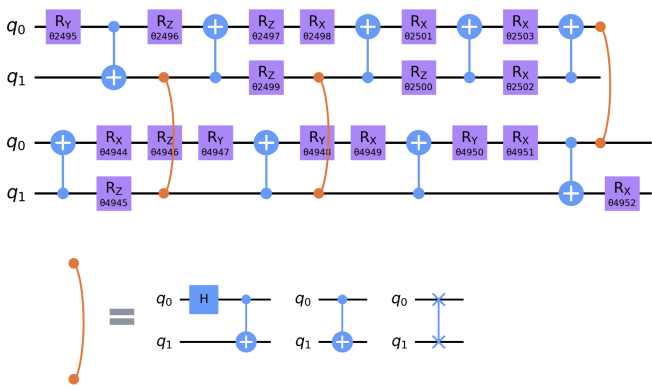


Fig. 8: We propose to insert two-qubit gates to mitigate the problem that sub-circuits do not interact with each other. Illustrated here are the possible options.

is reached. The details are described in Algorithm 2. We demonstrate an example in Figure 7.

### B. Stitching Sub-circuits

Since the sub-circuits in the library are limited in terms of depth and width. The expected global entanglement of the topology-aware ansatz may not reach the expectation. To fix this problem, we propose to use “stitching circuits” to boost the performance of the entire circuit. The stitching circuits are two-qubit gates that can enhance the entanglement.  $\{CNOT, CRX, SWAP\}$  and other two-qubit circuits can serve as stitching circuits. We apply the stitching circuits to places where the qubit is idle or at the end of the sub-circuits, as shown in Figure 8.

### C. Growing Circuit During Training

As shown in Algorithm 1, sub-circuits are classified into two groups. The sub-circuits in one group have an identity unitary matrix when parameters are set to zeros, and the rest form the other group. The purpose of grouping is to dynamically

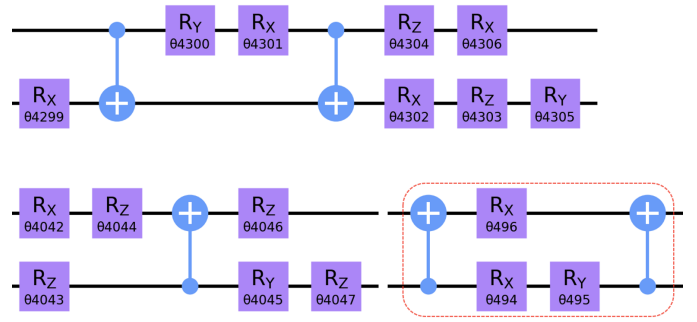


Fig. 9: During the training process, we propose to insert small sub-circuits at the end of the ansatz. The unitary matrix of this small ansatz is identity matrix if the parameters are initialized to zeros. Hence, the gradients of all the other parameters will not be abruptly changed.

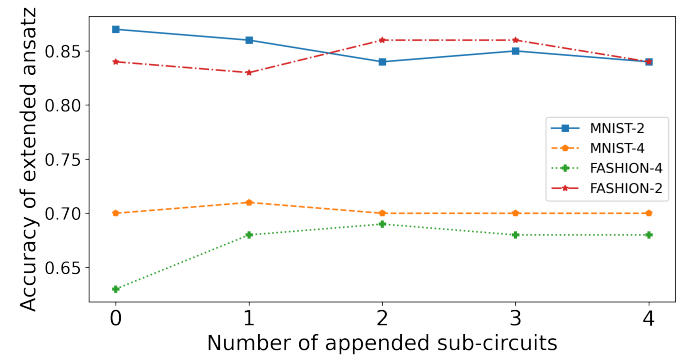


Fig. 10: The model accuracy varies with different numbers of appended sub-circuits.

“grow” the ansatz if it has inferior performance. In the process of training, we append the sub-circuits from the first group to ansatz. Since they are identity matrices in the beginning, the training loss of the appended ansatz will be smooth without abrupt changes. In this way, we can tell if the incremental addition is effective by observing the training loss in the first few iterations. This strategy allows us to refine the ansatz and boost its performance incrementally. The growing process ends if the model accuracy is not improved. Figure 9 provides an example, in which the sub-circuit inside the rectangular is appended to the ansatz. Figure 10 shows how accuracy changes with the number of appended sub-circuits. For different data sets (details in Section VI), we can see that there is always a sweet spot where the ansatz capacity is improved, while the optimizer can still handle the additional parameters. We observe a slight drop of accuracy as the number of appended sub-circuits further increases. We hypothesize that it is because the optimizer cannot handle too many additional parameters with limited iterations.

### D. Dynamic Gate Pruning

During the training process, some parameterized gates can be pruned according to the absolute values of the parameters.

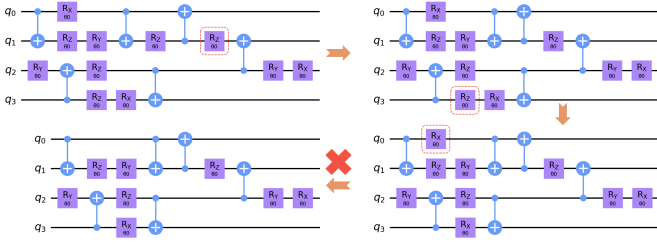


Fig. 11: Dynamic gate pruning will remove the gates with parameters that are close to zeros. The model accuracy for these ansatz are [0.80, 0.81, 0.80, 0.75]. The removal of the first two gates does not affect the model accuracy, while the removal of the last gate results in obvious accuracy drop.

If the parameter of the gate is close to zero, we will prune the parameterized gate and monitor the change in accuracy. The pruning process ends if a sharp drop of accuracy is observed. A trade-off exists between the pruning and the overall accuracy. Figure 11 illustrates an example of the ansatz before and after pruning. We can see that two out of 11 rotation gates are removed from the original ansatz. The gate pruning terminates at this point since further reduction of parameterized gates would result in a 5% decrease of accuracy (from 80% to 75%). In comparison, the removal of the first two parameterized gates leads to no reduction in model accuracy. Even though the ansatz is small, it achieves a classification accuracy of 81% for the two-class MNIST problem. It validates the great potentials of QNN algorithms: quantum circuits with strong capability to represent data.

## VI. EVALUATION

### A. Datasets and Backend Configuration

There are many datasets for the evaluation of classical machine learning algorithms. However, such datasets are usually large and too complicated for QNN algorithms. To evaluate the QNN circuits that are generated with our bottom-up methods, we adopt the datasets used in [36] and [82]. The datasets from [36] is composed of nine tasks of increasing difficulty but of suitable size. Each dataset contains a total of 1500 data points for training, testing and validation. The datasets from [82], on the other hand, are adopted from real-world applications such as MNIST [19], FASHION-MNIST [88] and VOWEL [20]. The input images from MNIST and FASHION are cropped to  $24 \times 24$  and down-sampled to  $4 \times 4$  with average pooling. Inputs from VOWEL are reduced to contain 10 features. Measurements of ansatz are conducted on Pauli-z basis to obtain the expectation values for each qubit. Then softmax is applied to produce probability values for different classes. As for backends, we use torch quantum [82] to perform simulations on classical computers. Even though our ansatz are generated based on the topology of IBM’s quantum devices [1], they are fine-grained enough to fit other kinds of backends such as trapped ion quantum computers. Experiments on real-world quantum computers are conducted on

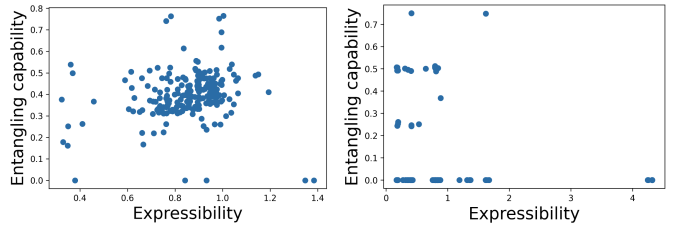


Fig. 12: The scatter plots show the relationship between expressibility and entangling capability. The right plot is generated for sub-circuits with less than five gates, while the sub-circuits in the left plot contain around 10 gates each. If the sub-circuits are too small, the search space for “good” ansatz will also be very limited.

IBM’s quantum computers such as `ibmq_quito` and `ibmq_lima`. Further details will be discussed in subsection VI-E.

### B. Sub-circuits Generation

The first step of our bottom-up approach is to create a large number of sub-circuits and evaluate them. Some example circuits and the values of corresponding criteria are shown in Figure 6. When we generate the sub-circuits, the size of the sub-circuits is limited. If the sub-circuits are too small, they cannot thoroughly explore the Hilbert Space with varying parameters. Figure 12 demonstrates the situation where small sub-circuits result in minimum search space. On the other hand, if the sub-circuits are too large, it obeys our principles to narrow down the design space.

### C. Performance of Combined Sub-circuit

The topology-aware ansatz is generated by combining sub-circuits with the best criteria. There are several ways to select the sub-circuits with “good” properties. We denote the sub-circuits with the best expressibility as “EXP” and the sub-circuits with the best entangling capability as “ENT”. We propose different ways to select the sub-circuits: EXP only, ENT only, ENT+EXP mixed. The baseline is marked as “random” and it is a randomly generated ansatz of similar size. [36] claims that strong correlation exists between classification accuracy and expressibility. At the same time, weak correlation exists between the accuracy and the entangling capability. Figure 13 validates this claim. The average accuracy for different policies are [0.52, 0.54, 0.57, 0.65]. Our initial ansatz achieves an average accuracy improvement of 13% compared with random ansatz over nine datasets. It confirms that the selected sub-circuits perform better than random sub-circuits.

### D. Effectiveness of Optimizations

Figure 14 shows the model accuracy of our ansatz at different optimization stage. We see that the topology-aware ansatz performs better than the manually designed ansatz [70]. For datasets {1a,1b,1c,2a,2b,2c,3a,3b,3c} adopted from [36], we notice a slight drop of accuracy after applying the optimization methods. It indicates that the initial ansatz is already sufficient for such tasks. The initial ansatz show an average 8.6%

TABLE I: Ansatz size comparison

	Depth	#Gates	#Params	Avg accuracy	Compiled depth	Compiled #gates	Compiled #CNOT gates
Base_1	5	11	8	0.54	12	30	3
Base_2	6	19	19	0.56	26	66	6
Base_3	5	11	4	0.61	20	40	3
Base_4	6	15	12	0.72	18	39	3
Base_5	9	16	16	0.74	49	83	16
Base_6	9	16	16	0.74	95	140	34
Base_7	9	16	8	0.51	31	55	16
Base_8	6	12	12	0.64	54	77	17
Base_avg	6.9	14.3	11.9	0.63	38	66.3	12.3
Initial ansatz	6	12	9	0.73	21	34	3
Stitched ansatz	6	13	9	0.71	18	32	4
Grown ansatz	6 to 7	13 to 17	9 to 12	0.68	18 to 22	32 to 45	4
Pruned ansatz	7	13 to 15	9 to 10	0.7	18 to 20	32 to 40	4

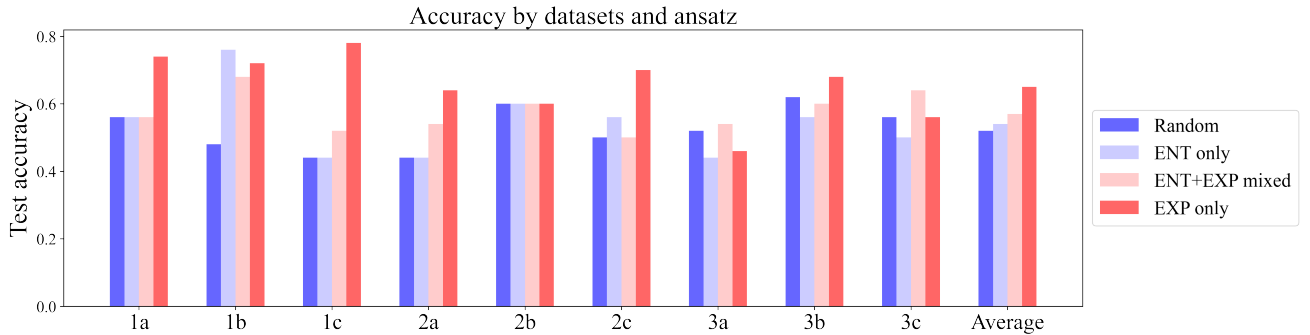


Fig. 13: Different ways to select the sub-circuits of top performance. ENT stands for sub-circuits with the best entangling capabilities (MW measure); EXP stands for sub-circuits with the best expressibility. We can see from the average accuracy that the expressibility is more correlated to the model accuracy.

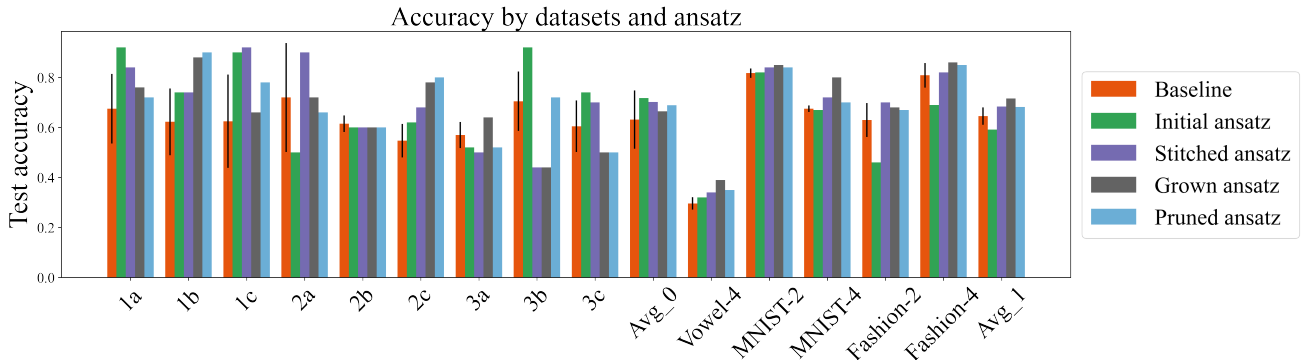


Fig. 14: The model accuracy at different stages of optimization. Avg\_0 and Avg\_1 stand for averaged results for datasets from [36] and [82] respectively.

advantage over manually-designed ansatz and 13% advantage over random ansatz in terms of model accuracy. In contrast, for datasets from [82] {MNIST-2, MNIST-4, FASHION-2, FASHION-4, VOWEL-4}, we see gradual improvement of model accuracy thanks to the incrementally built ansatz; and the grown ansatz provide an average 7.1% advantage of accuracy. We believe that the difference in problem size causes such phenomenon.

For machine learning tasks of more complexity such as {MNIST-4, FASHION-4, VOWEL-4}, the ansatz is larger before accuracy reaches saturation, which is also reflected in Figure 10. Since the ansatz generated by our approach is directly compatible with the hardware topology, we expect they have smaller size after they are compiled. The Table I shows that before the compilation process, the size of our ansatz is comparable with the manually-designed ansatz. But

TABLE II: Model Accuracy on Different Backends including Non-optimal Initial Layout (NOIL) Results

	MNIST-2	NOIL	MNIST-4	NOIL	FASHION-2	NOIL	FASHION-4	NOIL	Avg	NOIL
noise-free sim	0.85	N/A	0.76	N/A	0.84	N/A	0.67	N/A	0.78	N/A
ibmq_quito	0.86	0.87	0.71	0.63	0.84	0.80	0.69	0.65	0.78	0.74
ibmq_lima	0.86	0.71	0.76	0.67	0.83	0.83	0.68	0.67	0.78	0.72
ibmq_oslo	0.87	0.58	0.75	0.31	0.84	0.77	0.65	0.50	0.78	0.54

after the circuits are compiled onto quantum computers, our circuits are smaller due to its topology-aware nature. Overall, we achieve a depth reduction around 50% and a CNOT reduction up to 75%. Considering the fact that CNOT gates generally takes longer than the single-qubit gates on quantum computers. The circuit latency reduction is in fact more than 50%.

### E. Results on Real-world Quantum Computers

We test the trained ansatz on IBM’s cloud quantum computers. Table II displays different classification accuracy from various backends. Due to the limited size of our designed ansatz circuits, the classification accuracy with real machines are almost identical with the results collected on noise-free simulator. The columns with “NOIL” represent the accuracy results with the same ansatz but non-optimal initial layout (NOIL), where extra SWAP gates are needed. We insert such mismatch between our ansatz and hardware topology to investigate the affects of extra SWAP gates. For quantum computers (ibmq\_quito) with lower noise, the mismatch introduced slight drops in accuracy. However, it shows sharp decrease of accuracy when tested on quantum devices with higher noise (ibmq\_oslo). The difference emphasizes the importance of topology-aware techniques in the NISQ era, where quantum devices are prone to high gate errors. On average, TopGen shows accuracy advantages by 17% over the NOIL results.

### F. Overhead, Scalability and Barren Plateaus

The evaluation of sub-circuits is off-line and it only needs to be done once. After the sub-circuits are evaluated, the selection and combination of sub-circuits can be completed with negligible time. Therefore, the run-time overhead of our bottom-up approach based on the current quantum computers to create QNN ansatz is very low. As for the training overhead, since we adopt the “growing” method, the architecture search for the ansatz will happen during the training process. Under the ansatz of similar size, our overhead is smaller compared with methods where ansatz needs to be re-trained after the structure is determined. On the other side, we expect to see quantum computers of more than one thousand qubits in the next decade [14]. While these large computers are likely to have sparser connections, the graph based on their hardware topology can always be divided into smaller sub-graphs. The major overhead of our bottom-up approach comes from sub-circuits’ evaluation, which only scales with the size of sub-circuits. Therefore, the proposed bottom-up approach has high scalability and will work well on large quantum computers.

Moreover, recent work [30] suggests that, ADAPT-VQE, a well-designed ansatz [32] can naturally preclude the affects from barren plateaus and large numbers of local minima. When additional operators are appended to the ansatz, it is likely to create a deeper trap to “burrow” towards the exact solution. This explains why our idea of incrementally growing ansatz works, which is also confirmed in the results.

## VII. RELATED WORK

QML offers various potential applications for small quantum computers [10], [11], [13], [21], [22], [50], [58], [64]–[67]. In recent years, different structures of QNN have been proposed and tested [38], [52], [59], [81]. These works focus on maximizing the accuracy of quantum models for machine learning tasks. At the same time, the quantum compilers have made breakthroughs as well [8], [28], [48], [68], [73]. Better algorithms for qubit mapping and program synthesis have been proposed [35], [37], [46], [47], [57], [91]. Some papers [75], [87] propose to optimize the synthesis process with the information of hardware topology. However, they target general quantum programs, where the design space is not large. For QNN algorithms, intensive research has been conducted on finding the optimal ansatz [4], [56], [82]–[84], [90].

## VIII. CONCLUSION

In this paper, we propose a bottom-up approach to generate topology-aware ansatz for Variational Quantum Algorithms and we use the important Quantum Neural Networks as the benchmark to evaluate our method. The effectiveness of this approach is due to the flexibility of QNN ansatz. Because the minimized ansatz does not have physical meaning, the final states of the ansatz can be from the full Hilbert Space. To make the search tractable, we propose to first generate hardware compatible sub-circuits with “good” properties first, then combine the sub-circuits to form the initial ansatz. We propose several optimizations to compensate for the sparser qubit connection in the initially generated ansatz and increase accuracy. With this approach, the search of a huge design space is reduced to finding better sub-circuits that can form the high quality ansatz. We evaluated our approach with 14 data sets used in recent works. The results show that the ansatz generated by our solution achieves decent model accuracy with ansatz that are 50% smaller in depth. TopGen on three real machines demonstrates on average 17% higher accuracy.

## REFERENCES

- [1] <https://www.research.ibm.com/ibm-q/technology/devices/>.
- [2] Amira Abbas, David Sutter, Christa Zoufal, Aurélien Lucchi, Alessio Figalli, and Stefan Woerner. The power of quantum neural networks. *Nature Computational Science*, 1(6):403–409, 2021.
- [3] Dorit Aharonov and Michael Ben-Or. Fault-tolerant quantum computation with constant error rate. *SIAM Journal on Computing*, 2008.
- [4] Mahabubul Alam, Satwik Kundo, Rasit Onur Topaloglu, and Swaroop Ghosh. Quantum-classical hybrid machine learning for image classification (iccad special session paper). *arXiv preprint arXiv:2109.02862*, 2021.
- [5] Gadi Aleksandrowicz, Thomas Alexander, P Barkoutsos, L Bello, Y Ben-Haim, D Bucher, FJ Cabrera-Hernández, J Carballo-Franquis, A Chen, CF Chen, et al. Qiskit: An open-source framework for quantum computing. *Accessed on: Mar, 16, 2019*.
- [6] Yuri Alexeev, Dave Bacon, Kenneth R Brown, Robert Calderbank, Lincoln D Carr, Frederic T Chong, Brian DeMarco, Dirk Englund, Edward Farhi, Bill Fefferman, et al. Quantum computer systems for scientific discovery. *PRX Quantum*, 2(1):017001, 2021.
- [7] Rodney J Bartlett and Monika Musiał. Coupled-cluster theory in quantum chemistry. *Reviews of Modern Physics*, 79(1):291, 2007.
- [8] KOEN Bertels, Aritra Sarkar, Thomas Hubregtsen, M Serrao, Abid A Moueddenne, Amitabh Yadav, A Krol, and Imran Ashraf. Quantum computer architecture: Towards full-stack quantum accelerators. In *2020 Design, Automation & Test in Europe Conference & Exhibition (DATE)*, pages 1–6. IEEE, 2020.
- [9] Jacob Biamonte, Peter Wittek, Nicola Pancotti, Patrick Rebentrost, Nathan Wiebe, and Seth Lloyd. Quantum machine learning. *Nature*, 549(7671):195–202, 2017.
- [10] Alessandro Bisio, Giulio Chiribella, Giacomo Mauro D’Ariano, Stefano Facchini, and Paolo Perinotti. Optimal quantum learning of a unitary transformation. *Physical Review A*, 81(3):032324, 2010.
- [11] Alessandro Bisio, Giacomo Mauro D’Ariano, Paolo Perinotti, and Michal Sedláč. Quantum learning algorithms for quantum measurements. *Physics Letters A*, 375(39):3425–3434, 2011.
- [12] Gavin K Brennen. An observable measure of entanglement for pure states of multi-qubit systems. *arXiv preprint quant-ph/0305094*, 2003.
- [13] Jinglei Cheng, Haoqing Deng, and Xuehai Qia. Accqoc: Accelerating quantum optimal control based pulse generation. In *2020 ACM/IEEE 47th Annual International Symposium on Computer Architecture (ISCA)*, pages 543–555. IEEE, 2020.
- [14] Adrian Cho. Ibm promises 1000-qubit quantum computer—a milestone by 2023, 2020. URL <https://www.sciencemag.org/news/2020/09/ibm-promises-1000-qubit-quantum-computer-milestone-2023>, 2021.
- [15] John Clarke and Frank K Wilhelm. Superconducting quantum bits. *Nature*, 453(7198):1031–1042, 2008.
- [16] Gavin E Crooks. Gradients of parameterized quantum gates using the parameter-shift rule and gate decomposition. *arXiv preprint arXiv:1905.13311*, 2019.
- [17] Andrew W Cross, Lev S Bishop, Sarah Sheldon, Paul D Nation, and Jay M Gambetta. Validating quantum computers using randomized model circuits. *Physical Review A*, 100(3):032328, 2019.
- [18] Andrew W Cross, Lev S Bishop, John A Smolin, and Jay M Gambetta. Open quantum assembly language. *arXiv preprint arXiv:1707.03429*, 2017.
- [19] Li Deng. The mnist database of handwritten digit images for machine learning research. *IEEE Signal Processing Magazine*, 29(6):141–142, 2012.
- [20] Dheeru Dua and Casey Graff. UCI machine learning repository, 2017.
- [21] Vedran Dunjko, Nicolai Friis, and Hans J Briegel. Quantum-enhanced deliberation of learning agents using trapped ions. *New Journal of Physics*, 17(2):023006, 2015.
- [22] Vedran Dunjko, Jacob M Taylor, and Hans J Briegel. Quantum-enhanced machine learning. *Physical review letters*, 117(13):130501, 2016.
- [23] Jens Eisert, Marcus Cramer, and Martin B Plenio. Colloquium: Area laws for the entanglement entropy. *Reviews of modern physics*, 82(1):277, 2010.
- [24] Edward Farhi, Jeffrey Goldstone, and Sam Gutmann. A quantum approximate optimization algorithm. *arXiv preprint arXiv:1411.4028*, 2014.
- [25] Diego García-Martín and Germán Sierra. Five experimental tests on the 5-qubit ibm quantum computer. *arXiv preprint arXiv:1712.05642*, 2017.
- [26] Michael R Geller. Sampling and scrambling on a chain of superconducting qubits. *Physical Review Applied*, 10(2):024052, 2018.
- [27] Elizabeth Gibney. Hello quantum world! google publishes landmark quantum supremacy claim. *Nature*, 574(7779):461–463, 2019.
- [28] Pranav Gokhale, Ali Javadi-Abhari, Nathan Earnest, Yunong Shi, and Frederic T Chong. Optimized quantum compilation for near-term algorithms with openpulse. In *2020 53rd Annual IEEE/ACM International Symposium on Microarchitecture (MICRO)*, pages 186–200. IEEE, 2020.
- [29] Harper R Grimsley, George S Barron, Edwin Barnes, Sophia E Economou, and Nicholas J Mayhall. Adapt-vqe is insensitive to rough parameter landscapes and barren plateaus. *arXiv preprint arXiv:2204.07179*, 2022.
- [30] Harper R Grimsley, George S Barron, Edwin Barnes, Sophia E Economou, and Nicholas J Mayhall. Adapt-vqe is insensitive to rough parameter landscapes and barren plateaus, 2022.
- [31] Harper R Grimsley, Daniel Claudino, Sophia E Economou, Edwin Barnes, and Nicholas J Mayhall. Is the trotterized ucsd ansatz chemically well-defined? *Journal of chemical theory and computation*, 16(1):1–6, 2019.
- [32] Harper R Grimsley, Sophia E Economou, Edwin Barnes, and Nicholas J Mayhall. An adaptive variational algorithm for exact molecular simulations on a quantum computer. *Nature communications*, 10(1):1–9, 2019.
- [33] Lov K Grover. A fast quantum mechanical algorithm for database search. In *Proceedings of the twenty-eighth annual ACM symposium on Theory of computing*, pages 212–219, 1996.
- [34] Wen Guan, Gabriel Perdue, Arthur Pesah, Maria Schuld, Koji Terashi, Sofia Vallecorsa, and Jean-Roch Vlimant. Quantum machine learning in high energy physics. *Machine Learning: Science and Technology*, 2(1):011003, 2021.
- [35] Stefan Hillmich, Alwin Zulehner, and Robert Wille. Exploiting quantum teleportation in quantum circuit mapping. In *2021 26th Asia and South Pacific Design Automation Conference (ASP-DAC)*, pages 792–797. IEEE, 2021.
- [36] Thomas Hubregtsen, Josef Pichlmeier, Patrick Stecher, and Koen Bertels. Evaluation of parameterized quantum circuits: on the relation between classification accuracy, expressibility, and entangling capability. *Quantum Machine Intelligence*, 3(1):1–19, 2021.
- [37] Toshinari Itoko, Rudy Raymond, Takashi Imamichi, and Atsushi Matsuo. Optimization of quantum circuit mapping using gate transformation and commutation. *Integration*, 70:43–50, 2020.
- [38] Ben Jaderberg, Lewis W Anderson, Weidi Xie, Samuel Albanie, Martin Kiffner, and Dieter Jaksch. Quantum self-supervised learning. *arXiv preprint arXiv:2103.14653*, 2021.
- [39] Peter D. Johnson, Jonathan Romero, Jonathan Olson, Yudong Cao, and Alán Aspuru-Guzik. Qvector: an algorithm for device-tailored quantum error correction, 2017.
- [40] Jonathan A Jones, Michele Mosca, and Rasmus H Hansen. Implementation of a quantum search algorithm on a quantum computer. *Nature*, 393(6683):344–346, 1998.
- [41] Abhinav Kandala, Antonio Mezzacapo, Kristan Temme, Maika Takita, Markus Brink, Jerry M Chow, and Jay M Gambetta. Hardware-efficient variational quantum eigensolver for small molecules and quantum magnets. *Nature*, 549(7671):242–246, 2017.
- [42] Bruce E Kane. A silicon-based nuclear spin quantum computer. *nature*, 393(6681):133–137, 1998.
- [43] Ivan Kassal, James D Whitfield, Alejandro Perdomo-Ortiz, Man-Hong Yung, and Alán Aspuru-Guzik. Simulating chemistry using quantum computers. *Annual review of physical chemistry*, 62:185–207, 2011.
- [44] Solomon Kullback and Richard A Leibler. On information and sufficiency. *The annals of mathematical statistics*, 22(1):79–86, 1951.
- [45] Benjamin P Lanyon, James D Whitfield, Geoff G Gillett, Michael E Goggin, Marcelo P Almeida, Ivan Kassal, Jacob D Biamonte, Masoud Mohseni, Ben J Powell, Marco Barbieri, et al. Towards quantum chemistry on a quantum computer. *Nature chemistry*, 2(2):106–111, 2010.
- [46] Lingling Lao, Hans van Someren, Imran Ashraf, and Carmen G Al-mudever. Timing and resource-aware mapping of quantum circuits to superconducting processors. *IEEE Transactions on Computer-Aided Design of Integrated Circuits and Systems*, 2021.
- [47] Gushu Li, Yufei Ding, and Yuan Xie. Tackling the qubit mapping problem for nisq-era quantum devices. In *Proceedings of the Twenty-Fourth International Conference on Architectural Support for Programming Languages and Operating Systems*, pages 1001–1014, 2019.

- [48] Gushu Li, Anbang Wu, Yunong Shi, Ali Javadi-Abhari, Yufei Ding, and Yuan Xie. On the co-design of quantum software and hardware. In *Proceedings of the Eight Annual ACM International Conference on Nanoscale Computing and Communication*, pages 1–7, 2021.
- [49] Zhiding Liang, Jinglei Cheng, Hang Ren, Hanrui Wang, Fei Hua, Yongshan Ding, Fred Chong, Song Han, Yiyu Shi, and Xuehai Qian. Pan: Pulse ansatz on nisy machines. *arXiv preprint arXiv:2208.01215*, 2022.
- [50] Zhiding Liang, Hanrui Wang, Jinglei Cheng, Yongshan Ding, Hang Ren, Xuehai Qian, Song Han, Weiwen Jiang, and Yiyu Shi. Variational quantum pulse learning. *arXiv preprint arXiv:2203.17267*, 2022.
- [51] Zhiding Liang, Zhepeng Wang, Junhuan Yang, Lei Yang, Yiyu Shi, and Weiwen Jiang. Can noise on qubits be learned in quantum neural network? a case study on quantumflow. In *2021 IEEE/ACM International Conference On Computer Aided Design (ICCAD)*, pages 1–7. IEEE, 2021.
- [52] Yunchao Liu, Srinivasan Arunachalam, and Kristan Temme. A rigorous and robust quantum speed-up in supervised machine learning. *Nature Physics*, 17(9):1013–1017, 2021.
- [53] Yuriy Makhlin, Gerd Scöhn, and Alexander Shnirman. Josephson-junction qubits with controlled couplings. *nature*, 398(6725):305–307, 1999.
- [54] Jarrod R McClean, Sergio Boixo, Vadim N Smelyanskiy, Ryan Babbush, and Hartmut Neven. Barren plateaus in quantum neural network training landscapes. *Nature communications*, 9(1):1–6, 2018.
- [55] David A Meyer and Nolan R Wallach. Global entanglement in multi-particle systems. *Journal of Mathematical Physics*, 43(9):4273–4278, 2002.
- [56] Nam Nguyen and Kwang-Chen Chen. Quantum embedding search for quantum machine learning. *arXiv preprint arXiv:2105.11853*, 2021.
- [57] Siyuan Niu, Adrien Suau, Gabriel Staffelbach, and Aida Todri-Sanial. A hardware-aware heuristic for the qubit mapping problem in the nisy era. *IEEE Transactions on Quantum Engineering*, 1:1–14, 2020.
- [58] Giuseppe Davide Paparo, Vedran Dunjko, Adi Makmal, Miguel Angel Martin-Delgado, and Hans J Briegel. Quantum speedup for active learning agents. *Physical Review X*, 4(3):031002, 2014.
- [59] Evan Peters, Joao Caldeira, Alan Ho, Stefan Leichenauer, Masoud Mohseni, Hartmut Neven, Panagiotis Spentzouris, Doug Strain, and Gabriel N Perdue. Machine learning of high dimensional data on a noisy quantum processor. *arXiv preprint arXiv:2101.09581*, 2021.
- [60] Hieu Pham, Melody Guan, Barret Zoph, Quoc Le, and Jeff Dean. Efficient neural architecture search via parameters sharing. In *International conference on machine learning*, pages 4095–4104. PMLR, 2018.
- [61] Frank Phillipson. Quantum machine learning: Benefits and practical examples. In *QANSWER*, pages 51–56, 2020.
- [62] John Preskill. Quantum computing in the nisy era and beyond. *Quantum*, 2:79, 2018.
- [63] Sankar Das Sarma, Dong-Ling Deng, and Lu-Ming Duan. Machine learning meets quantum physics. *arXiv preprint arXiv:1903.03516*, 2019.
- [64] Masahide Sasaki, Alberto Carlini, and Richard Jozsa. Quantum template matching. *Physical Review A*, 64(2):022317, 2001.
- [65] Gael Sentís, Emilio Bagan, John Calsamiglia, Giulio Chiribella, and Ramon Muñoz-Tapia. Quantum change point. *Physical review letters*, 117(15):150502, 2016.
- [66] Gael Sentís, John Calsamiglia, Ramón Muñoz-Tapia, and Emilio Bagan. Quantum learning without quantum memory. *Scientific reports*, 2(1):1–8, 2012.
- [67] Gael Sentís, Mădălin Guță, and Gerardo Adesso. Quantum learning of coherent states. *EPJ Quantum Technology*, 2(1):1–22, 2015.
- [68] Yunong Shi, Nelson Leung, Pranav Gokhale, Zane Rossi, David I Schuster, Henry Hoffmann, and Frederic T Chong. Optimized compilation of aggregated instructions for realistic quantum computers. In *Proceedings of the Twenty-Fourth International Conference on Architectural Support for Programming Languages and Operating Systems*, pages 1031–1044, 2019.
- [69] Peter W Shor. Polynomial-time algorithms for prime factorization and discrete logarithms on a quantum computer. *SIAM review*, 41(2):303–332, 1999.
- [70] Sukin Sim, Peter D Johnson, and Alán Aspuru-Guzik. Expressibility and entangling capability of parameterized quantum circuits for hybrid quantum-classical algorithms. *Advanced Quantum Technologies*, 2(12):1900070, 2019.
- [71] Sukin Sim, Jonathan Romero, Jérôme F Gonthier, and Alexander A Kunitsa. Adaptive pruning-based optimization of parameterized quantum circuits. *Quantum Science and Technology*, 6(2):025019, 2021.
- [72] S Somaroo, CH Tseng, TF Havel, Raymond Laflamme, and David G Cory. Quantum simulations on a quantum computer. *Physical review letters*, 82(26):5381, 1999.
- [73] Damian S Steiger, Thomas Häner, and Matthias Troyer. Projectq: an open source software framework for quantum computing. *Quantum*, 2:49, 2018.
- [74] Edwin Stoudenmire and David J Schwab. Supervised learning with tensor networks. *Advances in Neural Information Processing Systems*, 29, 2016.
- [75] Bochen Tan and Jason Cong. Optimality study of existing quantum computing layout synthesis tools. *IEEE Transactions on Computers*, 2020.
- [76] Ho Lun Tang, VO Shkolnikov, George S Barron, Harper R Grimsley, Nicholas J Mayhall, Edwin Barnes, and Sophia E Economou. qubit-adapt-vqe: An adaptive algorithm for constructing hardware-efficient ansätze on a quantum processor. *PRX Quantum*, 2(2):020310, 2021.
- [77] Supanut Thanasilp, Samson Wang, Nhat A Nghiem, Patrick J Coles, and Marco Cerezo. Subtleties in the trainability of quantum machine learning models. *arXiv preprint arXiv:2110.14753*, 2021.
- [78] Jules Tilly, Hongxiang Chen, Shuxiang Cao, Dario Picozzi, Kanav Setia, Ying Li, Edward Grant, Leonard Wossnig, Ivan Rungger, George H Booth, et al. The variational quantum eigensolver: a review of methods and best practices. *arXiv preprint arXiv:2111.05176*, 2021.
- [79] Teague Tomesh, Kaiwen Gui, Pranav Gokhale, Yunong Shi, Frederic T Chong, Margaret Martonosi, and Martin Suchara. Optimized quantum program execution ordering to mitigate errors in simulations of quantum systems. In *2021 International Conference on Rebooting Computing (ICRC)*, pages 1–13. IEEE, 2021.
- [80] John S Van Dyke, George S Barron, Nicholas J Mayhall, Edwin Barnes, and Sophia E Economou. Scaling adaptive quantum simulation algorithms via operator pool tiling. *arXiv e-prints*, pages arXiv–2206, 2022.
- [81] Michael L Wall and Giuseppe D’Aguanno. Tree tensor network classifiers for machine learning: from quantum-inspired to quantum-assisted. *arXiv preprint arXiv:2104.02249*, 2021.
- [82] Hanrui Wang, Yongshan Ding, Jiaqi Gu, Yujun Lin, David Z Pan, Frederic T Chong, and Song Han. Quantumnas: Noise-adaptive search for robust quantum circuits. *arXiv preprint arXiv:2107.10845*, 2021.
- [83] Hanrui Wang, Jiaqi Gu, Yongshan Ding, Zirui Li, Frederic T Chong, David Z Pan, and Song Han. Roqnn: Noise-aware training for robust quantum neural networks. *arXiv preprint arXiv:2110.11331*, 2021.
- [84] Hanrui Wang, Zirui Li, Jiaqi Gu, Yongshan Ding, David Z Pan, and Song Han. On-chip qnn: Towards efficient on-chip training of quantum neural networks. *arXiv preprint arXiv:2202.13239*, 2022.
- [85] CM Wilson, JS Otterbach, Nikolas Tezak, RS Smith, AM Polloreno, Peter J Karalekas, S Heidel, M Sohaib Alam, GE Crooks, and MP da Silva. Quantum kitchen sinks: An algorithm for machine learning on near-term quantum computers. *arXiv preprint arXiv:1806.08321*, 2018.
- [86] Sau Lan Wu, Jay Chan, Wen Guan, Shaojun Sun, Alex Wang, Chen Zhou, Miron Livny, Federico Carminati, Alberto Di Meglio, Andy CY Li, et al. Application of quantum machine learning using the quantum variational classifier method to high energy physics analysis at the lhc on ibm quantum computer simulator and hardware with 10 qubits. *Journal of Physics G: Nuclear and Particle Physics*, 48(12):125003, 2021.
- [87] Xin-Chuan Wu, Marc Grau Davis, Frederic T Chong, and Costin Iancu. Qgo: Scalable quantum circuit optimization using automated synthesis. *arXiv preprint arXiv:2012.09835*, 2020.
- [88] Han Xiao, Kashif Rasul, and Roland Vollgraf. Fashion-mnist: a novel image dataset for benchmarking machine learning algorithms. *arXiv preprint arXiv:1708.07747*, 2017.
- [89] Christof Zalka. Simulating quantum systems on a quantum computer. *Proceedings of the Royal Society of London. Series A: Mathematical, Physical and Engineering Sciences*, 454(1969):313–322, 1998.
- [90] Shi-Xin Zhang, Chang-Yu Hsieh, Shengyu Zhang, and Hong Yao. Neural predictor based quantum architecture search. *arXiv preprint arXiv:2103.06524*, 2021.
- [91] Alwin Zulehner, Alexandru Paler, and Robert Wille. An efficient methodology for mapping quantum circuits to the ibm qx architectures. *IEEE Transactions on Computer-Aided Design of Integrated Circuits and Systems*, 38(7):1226–1236, 2018.